ACS Macro Letters

Letter

pubs.acs.org/macroletters

Evolutionary Optimization of Directed Self-Assembly of Triblock Copolymers on Chemically Patterned Substrates

Gurdaman S. Khaira,[†] Jian Qin,[†] Grant P. Garner,[†] Shisheng Xiong,[†] Lei Wan,[‡] Ricardo Ruiz,[‡] Heinrich M. Jaeger,[§] Paul F. Nealey,[†,∥] and Juan J. de Pablo*[,†,∥]

[†]Institute for Molecular Engineering, The University of Chicago, Chicago, Illinois 60637, United States

[‡]HGST, A Western Digital Company, San Jose, California 95135, United States

[§]James Franck Institute, The University of Chicago, Chicago, Illinois 60637, United States

[∥]Argonne National Laboratory, Argonne, Illinois 60439, United States

ABSTRACT: Directed self-assembly of block copolymers on chemical patterns is of considerable interest for sublithographic patterning. The concept of pattern interpolation, in which a subset of features patterned on a substrate is multiplied through the inherent morphology of an ordered block copolymer, has enabled fabrication of extremely small, defect-free features over large areas. One of the central challenges in design of pattern interpolation strategies is that of identifying system characteristics leading to ideal, defect-free directed assembly. In this work we demonstrate how a coarse-grained many-body model of block copolymers, coupled to an evolutionary computation (EC) strategy, can be used to design and optimize substrate−copolymer combinations for use in lithographic patterning. The proposed approach is shown to be significantly more effective than traditional algorithms based on random searches, and its results are validated in the context of recent experimental observations. The coupled simulation−evolution method introduced here provides a general and efficient method for potential design of complex device-oriented structures.

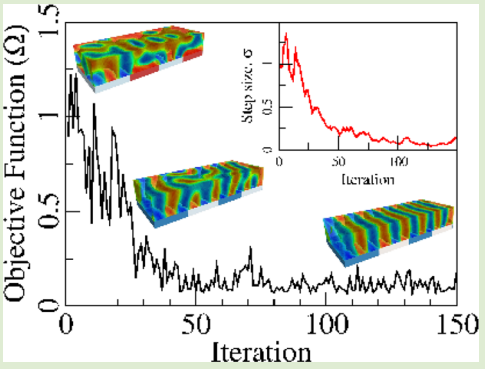

Block polymers exhibit a variety of ordered morphologies that are compatible with common geometrical features encountered in semiconductor devices, which are reaching dimensions on the order of tens of nanometers. At such length scales, directed self-assembly (DSA) of block polymers on chemical[1−3] or topographic patterns[4−6] provides a viable strategy for lithographic patterning.

In DSA on chemical patterns, which are the primary concern of this Letter, desirable features are created on a substrate through a combination of various traditional lithographic approaches; such features are then used to guide or direct the assembly of thin films of block polymers. Figure 1 shows a schematic representation of the underlying process for preparation of a lamellar morphology on a stripe-patterned substrate. Ideally, one of the stripes should interact preferentially with one of the blocks, and the other stripe should interact with the other block. To have ordered lamellae oriented perpendicular to the substrate, the interaction of both blocks with the air interface should be comparable. The figure corresponds to three-to-one (or 3X) patterning, where one feature on the surface corresponds to three features of the block copolymer morphology.

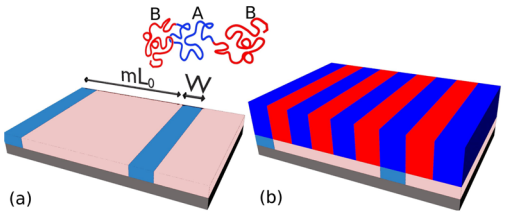

Figure 1. Schematic representation of *m*X density multiplication of block copolymers on chemical patterns. (a) Preferential stripes of width (W) are printed at pitch mL_0. (b) Increase in resolution due to block copolymer self-assembly with respect to the patterned substrate.

A particularly important concept in block copolymer DSA is that of pattern interpolation or density multiplication.[7−9] In that approach, only a subset number of features is created on the surface, and the block copolymer is used to fill in the gaps, thereby adding information into the overall assembly process. In that limit, the polymer can be viewed as a "smart" material that, with some guidance, can add features where they are needed. In the context of Figure 1, pattern interpolation would be achieved by using only half, one-third, or one-fourth of the substrate lines shown in the diagram. Furthermore, to facilitate fabrication, the features on the substrate could be larger than the characteristic dimensions of the block copolymer morphology (e.g., the lamellar period).[9]

Received: April 16, 2014
Accepted: July 9, 2014

   dx.doi.org/10.1021/mz5002349 | *ACS Macro Lett.* 2014, 3, 747−752

In this Letter, we focus on the creation of periodic lines, which currently represent one of the most promising geometrical features for insertion into patterning processes for commercial production of next-generation semiconductor devices and high-density storage media.[10] Figure 1(a) provides a schematic representation of the key design variables in pattern interpolation. They include the width W of the stripes, the characteristic period of the material (L_0), and the interaction of the blocks with the stripe and background regions of the substrate. These parameters are commonly determined by trial and error, where experiments with various combinations of the design variables are carried out until a suitable combination is identified. This approach becomes challenging and expensive as the number of variables increases. Recently, we proposed a covariance matrix adaptation evolution strategy (CMA-ES) which, when combined with a simple two-dimensional Ginzburg−Landau free energy and a Cahn−Hilliard approach, enabled design of substrates capable of guiding polymer assembly into desirable, nontrivial morphologies.[11] Importantly, this evolutionary strategy was shown to lead to much faster convergence than a simple random search approach.[12,13]

In this work, we address the question of whether an evolutionary strategy can in fact be used in combination with more realistic but also much more computationally demanding three-dimensional simulations of many-particle systems, where thermal fluctuations and molecular interactions are included, to design polymeric material systems with a target structure or functionality. We focus on the particular case of linear triblock BAB block copolymers (A and B label the monomer types) which, as shown in recent work, offer a promising alternative for fabrication of ultrasmall features relevant for applications[14,15] and are more tolerant to domain−pattern mismatch.[15] We examine their assembly into lamellae on stripe-patterned substrates. Our results indicate that the actual values of interactions between the polymer and the substrate depend on the degree of pattern interpolation and serve to demonstrate that the approach proposed here is much more efficient in finding such values than conventional algorithms based on random sampling of phase space (e.g., inverse Monte Carlo methods).

The description adopted here is based on the standard model of block copolymers, which has been used extensively to investigate the morphology of polymeric materials.[16] Past work has shown that such a model is able to reproduce the structure and thermodynamic properties of ordered block copolymer films on patterned substrates in quantitative agreement with experimental observations.[9,17,18] For brevity, only a brief account is given here. Readers are referred to the literature for additional details.[19] We consider systems of n BAB triblock copolymers, discretized into N beads connected by harmonic springs. The volume and temperature of the system are fixed at V and T, respectively. The total energy (H) of the system includes bonded, nonbonded, and substrate contributions. The polymer chains are assumed to be Gaussian; the bonded energy (H_b) is given by $\beta H_b = (3/2)\sum_{j=1}^{n_p}\sum_{i=1}^{N-1}(r_j(i+1) - r_j(i))^2/b^2$, where b is the statistical segment length, $r_j(i)$ the position of the ith segment of the jth chain, and $\beta^{-1} = k_BT$, where k_B is Boltzmann's constant.

The nonbonded energy is given by $\beta H_{nb} = \sqrt{N}\int_V (dr^3/R_e^3)[\chi N\phi_A\phi_B + (\kappa N/2)(1 - \phi_A - \phi_B)^2]$, where ϕ_A and ϕ_B denote the local densities of beads A and B, respectively; $R_e^2 = Nb^2$ is the mean square end-to-end distance; and $\sqrt{N} = \rho_0 R_e^3/N$ is the invariant degree of polymerization, where ρ_0 is the average bead density. The first term in the volume integral describes the repulsion between unlike monomers and is characterized by the Flory−Huggins parameter (χ). The second term represents the finite compressibility of the material, quantified by κ, which is proportional to the compression modulus.[20] In the implementation adopted here, the simulation domain is subdivided into cubic volume elements, and local densities (ϕ) are mapped onto the grid defined by those elements using a zeroth-order particle-to-mesh (PM) scheme.[19] Such an implementation allows for fast calculation of the nonbonded energy and has been shown to provide results in agreement with those of more elaborate interpolation schemes.[19,21]

As shown in Figure 1(a), a guiding stripe of width W, which is preferential to block A, is patterned at a pitch mL_0. The contribution of the pattern to the energy arising from a particle of type α at position r is given by a short-range potential of the form $\beta H_{ext}(r,\alpha) = ((\Lambda(\alpha))/d_s)\exp(-(r_z/2d_s)^2)$. Parameters $\Lambda(\alpha)$ and d_s denote the surface interaction strength for type α and its range, respectively. The perpendicular distance between the particle and the substrate is denoted by r_z. The strength of a guiding stripe for block A is given by $\Lambda(A) = \Lambda_s$. The remaining pattern area is filled with a background material having an affinity toward block A given by Λ_b. For simplicity, the surface interaction parameters are assumed to be symmetric, i.e., $\Lambda_s(A) = -\Lambda_s(B)$ and $\Lambda_b(A) = -\Lambda_b(B)$. Such an assumption has been shown to give an overall description of DSA in good agreement with experiments.[7,9,17,18]

The structure of the system is evolved by resorting to a Monte Carlo algorithm with Metropolis sampling. Trial displacements of molecules are accepted with probability $P_{acc} = \min(1,\exp(-\beta\Delta H))$, where ΔH corresponds to the change in energy induced by the displacement. One of the outputs of a simulation is a three-dimensional scalar field of the order parameter given by $\psi(r) = \langle(\phi_A(r) - \phi_B(r))/(\phi_A(r) + \phi_B(r))\rangle$, which we use to define "target" structures.

The covariance matrix adaptation evolution strategy (CMA-ES) belongs to a family of evolutionary computing algorithms where principles from biological evolution are adopted to find a set of variables that optimizes a chosen objective function.[22] It has been used in the context of materials research for optimization of packing problems[23] and for crystal structure prediction.[24] It is a stochastic and iterative method, where populations of distinct system samples are evolved according to the relevant dynamics, before assessment according to a fitness function is used to determine whether individual samples are terminated or allowed to multiply. At each iteration, a correlated sample population of size λ is generated based on information derived from previous iterations. The correlation among the population is governed by the covariance matrix ($\mathbf{C}$), and the search window size is dictated by the step size (σ); the λ "offspring" are then ranked according to the fitness function, and the best μ offspring are chosen to be used in the next iteration. A key feature of CMA-ES is its efficient protocol for mutation and recombination of offspring. In a simple random search, a new population is obtained by perturbing the old population using Gaussian noise. In contrast, CMA-ES uses the covariance matrix to perturb the system along specific search directions. The covariance matrix is adapted at each iteration step by "learning" from the "fitness" of the entire population. This helps control the diversity of the population and avoid premature convergence around a local optimum. For

dx.doi.org/10.1021/mz5002349 | ACS Macro Lett. 2014, 3, 747−752

additional information about the CMA-ES, the reader is referred to the literature.[25]

The target morphology considered here consists of defect-free perpendicular lamella. Our goal is to identify an optimal combination of the stripe width (W), guiding strength of the stripe (Λ_s(A)), and strength of the background brush (Λ_b(A)) leading to the target morphology on a stripe-patterned substrates. The objective function Ω that we choose to minimize is the mean-square-difference of the spatial order parameter between a given morphology ($\psi_i(r)$) and the target morphology ($\psi_{target}(r)$), i.e., $\Omega_i = (1/V)\int_V dr^3((\psi_i(r) - \psi_{target}(r))^2)^{1/2}$. The closer the value of Ω_i is to zero, the closer the morphology i is to the target. Let $\mathbf{X} = [W,\Lambda_s(A),\Lambda_b(A)]^T$ be the column vector representing the combination of variables to be optimized. The initial value of $\mathbf{X}$ is chosen at random. From this initial value (the initial mean), a normally distributed population of offsprings ($\mathbf{X}_i$; $i = 1, 2, ..., \lambda$) of size $\lambda = l$ is generated. In this work, we use $l = 31$. We then carry out λ independent Monte Carlo simulations, each with a corresponding $\mathbf{X}_i$ as an input. The output of each molecular simulation $\psi_i(r)$ is then used to calculate the objective function Ω_i. The λ offsprings are rank-ordered according to Ω_i, and a subset μ out of these survives into the next generation. Here we use $\mu = 4$. The chosen μ offspring are then used to calculate a new mean ($\bar{\mathbf{X}}$), covariance matrix ($\mathbf{C}$), and step size (σ),[25] and the process is repeated until convergence.

As mentioned earlier, we consider a symmetric and linear BAB triblock copolymer with $\sqrt{N} = 74$, $\chi N = 64$, and $\kappa N = 45$. The chain is discretized into 64 beads, with 32 beads of type A in the middle and 16 beads of type B connected to each side of the A block. These parameters correspond to a P2VP−PS−P2VP triblock copolymer with molecular weight 9K−18K−9K g/mol and periodicity $L_0 = 16.5$ nm, which has been shown to give good results in 3X multiplication experiments. The simulation domain considered here has dimensions $2mL_0 \times 3L_0 \times L_0$; each simulation is run for a sufficiently large number of Monte Carlo steps (200 000) to ensure that the block copolymer reaches the equilibrium state corresponding to the input $\mathbf{X}_i$.

In the context of 3X density multiplication, we seek the system parameters leading to defect-free perpendicular lamellae when guiding stripes are $3L_0$ apart. That is, one chemical stripe is used to guide three polymer lamellar domains. The target morphology consists of well-formed, rectangular lamellae perpendicular to the substrate. Note that, to assess finite-size effects, multiple independent simulations are also run without chemical patterns; defective lamella were obtained in all cases. Thus, for the system size considered here, "patterning" is required to direct the copolymers into defect-free perpendicular lamella.

Evolutionary CMA-ES iterations are carried out by varying the set of parameters $[W,\lambda_s(A),\lambda_b(A)]$ until convergence. Convergence is achieved when the step size (σ) of the CMA-ES reached a small number close to zero. A lower value of σ implies a smaller search window and indicates that the objective function and the guiding pattern's parameter fluctuate about their respective mean value. Figure 2 shows the value of Ω for the fittest offspring throughout the course of successive CMA-ES iterations. After approximately 30 iterations, CMA-ES is able to narrow down the region of interest and spends the rest of the time fine-tuning the pattern parameters required for optimal assembly. Several representative configurations corresponding to fit offspring at various stages of the simulation are also shown in the figure.

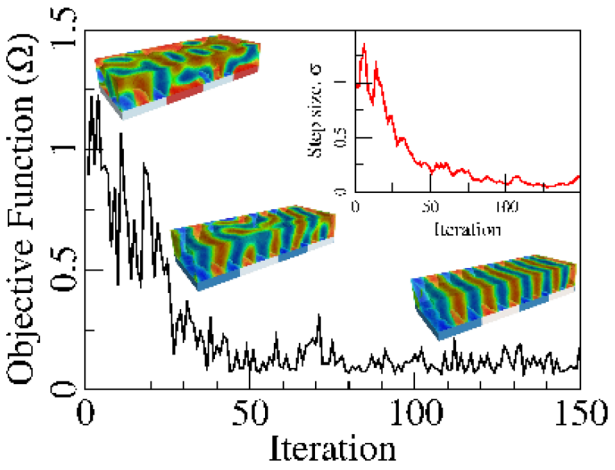

Figure 2. Value of the objective function corresponding to the best offspring as a function of CMA-ES iterations for 3X density multiplication. Adaptation of the search step size σ is shown in the inset.

Our results indicate that for density multiplication factors greater than 2 there are two regions of W/L_0, where defect-free perpendicular lamellae can form. The first, "trivial" regime corresponds to the optimum width of the guiding stripe, i.e., $W = 0.5L_0$. The second, potentially more interesting regime, corresponds to $W = 1.5L_0$. In the former case, only one lamellar domain sits on the guiding stripe, while in the latter, three lamellar domains sit on the guiding stripe. Two of these are preferential to the stripe (see Figure 1). The evolution of the pattern variables for these two regimes is shown in Figure 3.

The optimal strength of the guiding stripe for a defect-free assembly is different in each regime. For $W = 0.5L_0$, a strong preferential substrate ($\Lambda_s(A) = 1.54$) is predicted. In contrast, only a moderately preferential substrate ($\Lambda_s(A) = 0.34$) is predicted for $W = 1.5L_0$. For $0.5L_0$ guiding, the chemical stripes are narrow and are separated by $2.5L_0$; directing the defect-free assembly over these narrow stripes requires a strong anchoring of the preferential block to the guiding stripe. Note that the probability of defect formation increases for weaker patterns.[26] On the other hand, for $1.5L_0$ guiding, a moderate anchoring is sufficient to drive the assembly, as stripes are wider in area and closer to each other. Moreover, since one nonpreferential domain also sits on the guiding stripe, having too strong an anchoring for preferential blocks (and therefore a strong repulsion for nonpreferential blocks) would result in the formation of three-dimensional nonregular structures.[9]

The background strength for both cases is essentially neutral, with only a slight preference for the B block. The preference of the background for the B block is smaller for the $W = 0.5L_0$ case than for the $1.5L_0$ case because the surface coverage ratio of A blocks to B blocks on the background is higher in the former case. Note that Liu et al.[9] have observed this behavior in experiments and provided a thermodynamic argument to explain the neutrality of the background brush based on the surface coverage ratio of the blocks.

The results for 4X density multiplication are similar to those reported above for 3X in that the optimal widths of the guiding stripe are the same, i.e., $W = 0.5L_0$ or $W = 1.5L_0$. However, there are three important differences in the underlying chemical pattern parameters for 3X and 4X as shown in Figure 4(a).

dx.doi.org/10.1021/mz5002349 | ACS Macro Lett. 2014, 3, 747−752

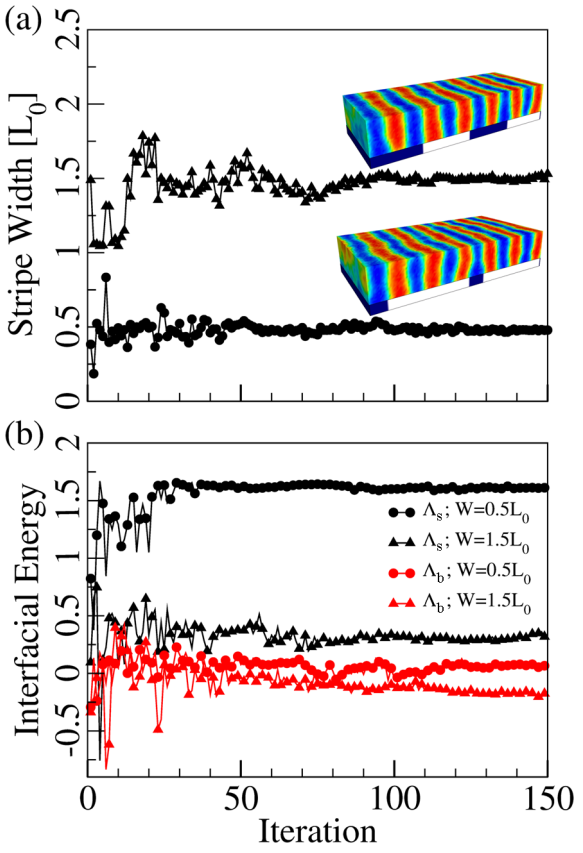

Figure 3. (a) Evolution of the stripe width W on 3X density multiplication for both $0.5L_0$ (circles) and $1.5L_0$ (triangles) regimes. The final equilibrium morphology corresponding to each regime is shown on top of each curve. (b) Corresponding evolution of Λ_s(A) and Λ_b(A) for both stripe widths.

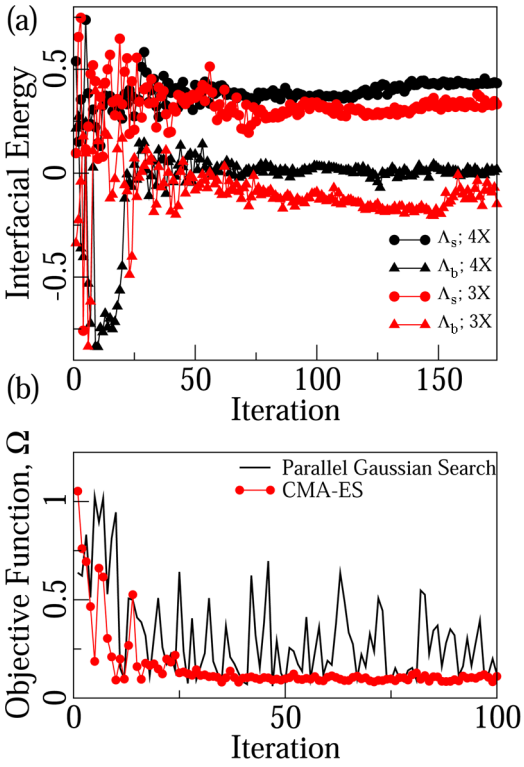

Figure 4. (a) Comparison of the interfacial energy parameters, Λ_s and Λ_b, for 4X and 3X density multiplication at $W = 1.5L_0$. (b) Objective function minimization by a parallel Gaussian search and the CMA-ES.

First, the optimal interaction of the stripe is predicted to be stronger for 4X (Λ_s(A) = 0.44 compared to Λ_s(A) = 0.34). This is due to the fact that the stripes are located further away in 4X density multiplication, which in turn requires stronger anchoring to register the preferential domains to the pattern. Second, the background in the 4X case is more neutral than in the 3X case, where it exhibited a slight preference for the B block. This can again be explained on the basis of the surface coverage ratio of block A to B on the background, which in the case of 4X with $W = 1.5L_0$ was 2:3, compared to 1:2 for 3X density multiplication. Third, the parameter fluctuations around their optimal values in the later stages of evolutionary computations are smaller in the 4X case than in the 3X case. This shows that 4X multiplication is less permissive than 3X, and a much narrower range of processing conditions leads to optimal assembly. Operationally, the objective function landscape is shallower in 3X around the converged variables, and the penalty for exploring parameter space around the minimum is smaller, thereby increasing the variance of the parameters sampled by the CMA-ES. It is worth pointing out that the same calculations reported here for triblocks can be performed on diblock copolymers. Our results (not shown) are comparable to those for triblocks, except that fluctuations of Λ are more pronounced in the initial stages of evolution. Here we reiterate that a key reason for using triblocks in this work is that they are more tolerant to domain pattern mismatch, as demonstrated by Ji et al.,[15] due to the fact that they can adopt either loop or bridge conformations (and thus be more flexible). This is particularly important for design of patterns with ultrasmall feature sizes.

Poly(2-vinylpyridine-styrene-*b*-2-vinylpyridine) (P2VP−PS−P2VP) of molecular weight 36.3 kg/mol was synthesized in our laboratory. Self-assembly of these triblock molecules was directed on chemical patterns according to the process flow described in ref 27. Briefly, a cross-linkable polystyrene (PS) mat of thickness 6−8 nm was deposited on a silicon wafer and further patterned by electron beam lithography to form PS-preferential lines. The width of the lines and their interaction chemistry were designed according to the guidelines provided by our hybrid evolutionary calculations for 3X and 4X multiplication, namely, $W = 1.5L_0$, and weak interactions between the stripes and the PS block. The remaining area was grafted by a random copolymer brush to create a background layer. Subsequently, a thin film of triblock copolymers was spin-coated on the chemical pattern, and the samples were allowed to anneal in the presence of acetone, which is a neutral solvent for both blocks. Under these conditions, the copolymers self-assembled into perpendicular lamellae with characteristic period L_0 = 16.5 nm. Figure 5 shows the top down SEM view of the underlying chemical patterns of stripe width $W = 1.5L_0$ for 3X (a) and 4X (b) density multiplication and the corresponding block copolymer assembly in (c) and (d), respectively. It is clear that sub 10 nm dimensions are accessible by using coarser guiding patterns that are easier to fabricate than thinner lines. The processing conditions that our evolutionary optimization scheme predicts lead to triblock copolymer assembly that is nearly perfectly registered on guiding stripes of width $W = 1.5L_0$ for both 3X and 4X multiplication. (The image shown in Figure 5 indicates that one can achieve defect-free assembly over areas encompassing

dx.doi.org/10.1021/mz5002349 | ACS Macro Lett. 2014, 3, 747−752

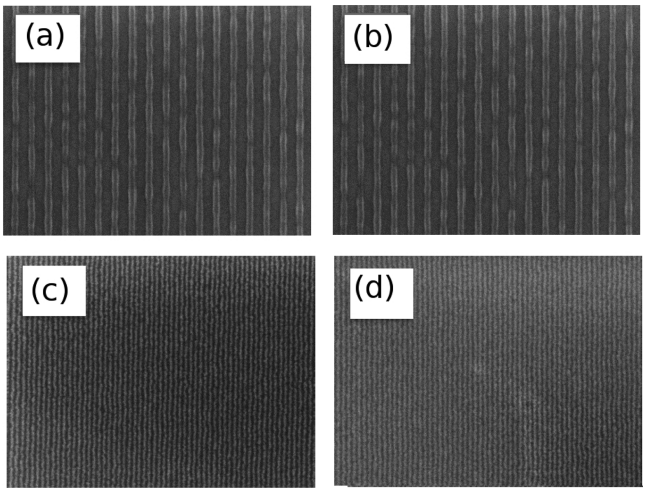

Figure 5. Underlying chemical patterns employed for directed assembly and final morphology of the P2VP−PS−P2VP triblock copolymer with molecular weight 9K−18K−9K g/mol assembled on those patterns. Results shown are for $W = 1.5L_o$ and $L_o = 24.5$ nm. (a) 3X and (b) 4X density multiplication. In both cases, triblock copolymers self-assemble into perpendicular lamellae with period 16.5 nm (c) and (d).

several microns. Whether defects arise over longer length scales has not been addressed by our calculations or experiments, and it is an issue that is intimately related to the kinetics of self-assembly, as discussed in other work.[14,28,29])

The most computationally demanding aspect of our evolutionary calculations is the molecular simulation required to find the equilibrium block copolymer morphology corresponding to each set of the pattern's parameters. The particle to mesh approach[19] adopted here takes approximately 1 h to find a local equilibrium, and the algorithm scales as $nN\log(nN)$. For each evolutionary iteration, the molecular simulations corresponding to each offspring can be run on parallel processors. This approach of testing multiple combinations of pattern variables simultaneously results in faster convergence compared to a sequential random search.[11] One possible improvement to a naive sequential search would be a parallel Gaussian random search, where at each iteration λ combinations of the variables are generated and μ best individuals are chosen after ranking them according to their corresponding objective function value. In contrast to CMA-ES, however, these λ combinations would be uncorrelated, and the search domain for each variable would be fixed. For completeness, in Figure 4(b) we compare the convergence behavior of CMA-ES with such a parallel Gaussian random search. Clearly, the CMA-ES is able to minimize the objective function in a much smaller number of iterations, showing that CMA-ES provides a considerable improvement over a conventional random search.

We have presented an efficient approach, based on a computational evolutionary strategy, to identify the necessary parameters or process variables required to direct the assembly of block copolymers into desirable target structures. We demonstrate this approach by optimizing the interaction parameters that lead to defect-free assembly of lamellar structures on guiding stripes. Monte Carlo simulations of fully three-dimensional polymeric systems, with fluctuations, were employed to predict the block copolymer morphology corresponding to a particular combination of pattern variables. The predictions of our simulations are consistent with recent experiments, which suggest that 3X and 4X interpolation of triblock copolymers is possible, provided the interaction of the stripes is carefully tuned according to the specifications identified in our calculations. Importantly, our combined computational and experimental strategy demonstrates unequivocally that DSA of triblock copolymers can be used to create defect-free sub-10 nm features, as required by lithographic approaches for fabrication of the next generation of semiconductor devices. While this work was focused on DSA of lines, the evolutionary strategy presented here can be used without need for modification for study of arbitrary patterns. A key finding of this Letter is the demonstration that such a strategy can in fact be used in conjunction with fully three-dimensional simulations of fluctuating systems to identify optimal conditions to achieve a target functionality.

AUTHOR INFORMATION

Corresponding Author

*E-mail: depablo@uchicago.edu.

Notes

The authors declare no competing financial interest.

ACKNOWLEDGMENTS

This work was performed under award 70NANB14H012 from U.S. Department of Commerce, National Institute of Standards and Technology as part of the Center for Hierarchical Material Design (CHiMaD). Additional support from the Semiconductor Research Corporation for development of new processing strategies for sublithographic patterning is gratefully acknowledged. H.M.J. acknowledges support from NSF CBET 1334426.

REFERENCES

(1) Kim, S. O.; Solak, H. H.; Stoykovich, M. P.; Ferrier, N. J.; de Pablo, J. J.; Nealey, P. F. *Nature* **2003**, *424*, 411−414.
(2) Stoykovich, M. P.; Müller, M.; Kim, S.; Solak, H.; Edwards, E.; de Pablo, J.; Nealey, P. *Science* **2005**, *308*, 1442.
(3) Stoykovich, M. P.; Kang, H.; Daoulas, K. C.; Liu, G.; Liu, C.-C.; de Pablo, J. J.; Müller, M.; Nealey, P. F. *ACS Nano* **2007**, *1*, 168−175.
(4) Rockford, L.; Liu, Y.; Mansky, P.; Russell, T.; Yoon, M.; Mochrie, S. *Phys. Rev. Lett.* **1999**, *82*, 2602.
(5) Segalman, R. A.; Yokoyama, H.; Kramer, E. J. *Adv. Mater.* **2001**, *13*, 1152−1155.
(6) Cheng, J. Y.; Mayes, A. M.; Ross, C. A. *Nat. Mater.* **2004**, *3*, 823−828.
(7) Ruiz, R.; Kang, H.; Detcheverry, F. A.; Dobisz, E.; Kercher, D. S.; Albrecht, T. R.; de Pablo, J. J.; Nealey, P. F. *Science* **2008**, *321*, 936−939.
(8) Cheng, J. Y.; Rettner, C. T.; Sanders, D. P.; Kim, H.-C.; Hinsberg, W. D. *Adv. Mater.* **2008**, *20*, 3155−3158.
(9) Liu, C.-C.; Ramírez-Hernández, A.; Han, E.; Craig, G. S. W.; Tada, Y.; Yoshida, H.; Kang, H.; Ji, S.; Gopalan, P.; de Pablo, J. J.; Nealey, P. F. *Macromolecules* **2013**, *46*, 1415−1424.
(10) http://www.itrs.net/Links/2011ITRS/2011Chapters/2011Lithography.pdf.
(11) Qin, J.; Khaira, G. S.; Su, Y.; Garner, G. P.; Miskin, M.; Jaeger, H. M.; de Pablo, J. J. *Soft Matter* **2013**, *9*, 11467−11472.
(12) Hannon, A. F.; Gotrik, K. W.; Ross, C. A.; Alexander-Katz, A. *ACS Macro Lett.* **2013**, *2*, 251−255.
(13) Hannon, A. F.; Ding, Y.; Bai, W.; Ross, C. A.; Alexander-Katz, A. *Nano Lett.* **2013**, *14*, 318−325.
(14) Nagpal, U.; Detcheverry, F. A.; Nealey, P. F.; de Pablo, J. J. *Macromolecules* **2011**, *44*, 5490−5497.

(15) Ji, S.; Nagpal, U.; Liu, G.; Delcambre, S. P.; Müller, M.; de Pablo, J. J.; Nealey, P. F. *ACS Nano* **2012**, *6*, 5440−5448.
(16) Helfand, E. *Macromolecules* **1975**, *8*, 552−556.
(17) Detcheverry, F. A.; Liu, G.; Nealey, P. F.; de Pablo, J. J. *Macromolecules* **2010**, *43*, 3446−3454.
(18) Liu, G.; Detcheverry, F.; Ramírez-Hernández, A.; Yoshida, H.; Tada, Y.; de Pablo, J. J.; Nealey, P. F. *Macromolecules* **2012**, *45*, 3986−3992.
(19) Detcheverry, F. A.; Kang, H.; Daoulas, K. C.; Müller, M.; Nealey, P. F.; de Pablo, J. J. *Macromolecules* **2008**, *41*, 4989−5001.
(20) Pike, D. Q.; Müller, M.; de Pablo, J. J. *J. Chem. Phys.* **2011**, *135*, 114904.
(21) Detcheverry, F. A.; Pike, D. Q.; Nealey, P. F.; Müller, M.; de Pablo, J. J. *Phys. Rev. Lett.* **2009**, *102*, 197801.
(22) Eiben, A. E.; Smith, J. E. *Introduction to evolutionary computing*; Springer: New York, 2003.
(23) Miskin, M. Z.; Jaeger, H. M. *Nat. Mater.* **2013**, *12*, 326−331.
(24) Oganov, A. R.; Lyakhov, A. O.; Valle, M. *Acc. Chem. Res.* **2011**, *44*, 227−237.
(25) Hansen, N.; Müller, S. D.; Koumoutsakos, P. *Evol. Comput.* **2003**, *11*, 1−18.
(26) Nagpal, U.; Müller, M.; de Pablo, J. J. *ACS Macro Lett.* **2012**, *1*, 418−422.
(27) Liu, C.-C.; Han, E.; Onses, M. S.; Thode, C. J.; Ji, S.; Gopalan, P.; Nealey, P. F. *Macromolecules* **2011**, *44*, 1876−1885.
(28) Welander, A. M.; Kang, H.; Stuen, K. O.; Solak, H. H.; Müller, M.; de Pablo, J. J.; Nealey, P. F. *Macromolecules* **2008**, *41*, 2759−2761.
(29) Takahashi, H.; Laachi, N.; Delaney, K. T.; Hur, S.; Weinheimer, C. J.; Shykind, D.; Fredrickson, G. H. *Macromolecules* **2012**, *45*, 6253−5265.